JACS
JOURNAL OF THE AMERICAN CHEMICAL SOCIETY
Article
pubs.acs.org/JACS

Energy Analysis of Aluminosilicate Zeolites with Comprehensive Ranges of Framework Topologies, Chemical Compositions, and Aluminum Distributions

Koki Muraoka, Watcharop Chaikittisilp,* and Tatsuya Okubo*

Department of Chemical System Engineering, The University of Tokyo, 7-3-1 Hongo, Bunkyo-ku, Tokyo 113-8656, Japan

Supporting Information

ABSTRACT: The contents and locations of Al in the zeolite frameworks are one of the key factors determining the physicochemical properties of zeolites. Systematic evaluation of the characteristics of zeolites with a wide variety of framework topologies, a wide range of Si/Al ratios, and various locations of Al is of great significance, but very challenging due to the limitation of the realizable ranges of Al contents in zeolites as well as the limited information on the Al locations obtained from the current analytical techniques. Here, we report the systematic analysis of the energetics of aluminosilicate zeolites with 209 existing framework topologies at different Si/Al ratios using molecular mechanics. More than 43 000 initial structures were generated to give comprehensive views of the energetics of zeolites. The results coincide well with the structural knowledge obtained experimentally. It was revealed that the relation between the relative framework energies versus the Al contents varies in accordance with the topologies, suggesting that the relative stability of zeolites depends not only on the topologies, but also on the substituting contents of Al. For particular topologies with the same Al contents, in addition, comparisons between random and specific distributions of Al showed that zeolite with Al at a particular T site is energetically more stable than those with random distributions, suggesting the inherent influences of the Al locations. The contents and locations of Al in zeolites likely have a certain preference that may reflect the range of chemical compositions, the Al distributions, and consequently the physicochemical properties of realizable aluminosilicate zeolites.

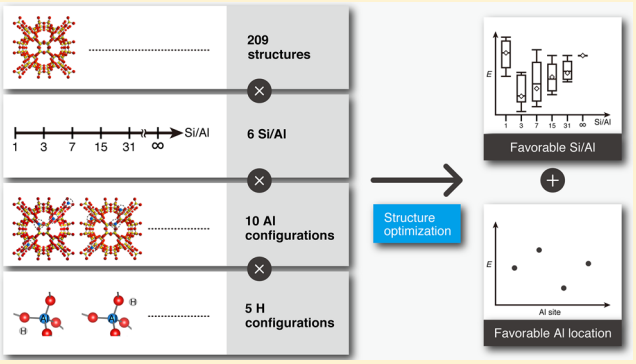

INTRODUCTION

Linking the structures and chemical compositions of framework materials to their intrinsic physicochemical properties is vital for understanding of the fundamental origins determining the material properties and functions. Such fundamental understanding can, therefore, provide an essential basis for material design. Zeolite is a class of crystalline microporous silica-based framework materials that has been utilized in a wide variety of real applications across chemical industries.[1−3] Framework structures of zeolites are built from corner-sharing, tetrahedrally coordinated $TO_{4/2}$ primary units (where T is a tetrahedral atom such as Si, Al, B, Ga, and Zn). In general, framework topology and chemical composition are the most fundamental descriptor reflecting the properties of zeolites. The framework topology is well-defined three-dimensional networks of $TO_{4/2}$ tetrahedra with more than 230 different topologies identified and assigned with three-letter codes by the International Zeolite Association (IZA),[4] among theoretically uncountable hypothetical candidates.[5−8] The information on crystallographic coordinates obtained from the topologies lets us describe the interior structure of zeolites. Due to the periodicity of the framework structures, the interior space is also periodic, thereby forming different uniform channel systems depending on the topologies.

While the topology gives rather the mathematical information related to space, the chemical composition gives the information on the physicochemical features. When Si at the tetrahedral site (T site) of the zeolite frameworks is substituted by di- or trivalent atoms with a typical substitute being Al, negative charges at oxygen surrounding the substituting atoms are generated, thereby yielding anionic silicate-based frameworks. With respect to utilization of zeolites, as a result, the locations of substitutes are of great importance because they are directly related to active sites, in particular, Brönsted acid sites when negative charges are counterbalanced by protons. In addition to protons, the counterions can be cationic transition metal species, possessing various structures and coordination, which can exhibit extraordinary redox behaviors for catalysis.

The general composition formula of anhydrous aluminosilicate zeolites can be expressed as $M^{n+}_{x/n}Al_xSi_{1-x}O_2$, where M is the counterion, n is the valence of M, and x is the substituting amount of Al ($x \leq 0.5$). Aluminosilicate zeolites with high Al substitutions exhibiting large ion-exchange capacity due to their high charge density are widely utilized as detergent builders and

Received: February 5, 2016
Published: April 20, 2016

DOI: 10.1021/jacs.6b01341
J. Am. Chem. Soc. 2016, 138, 6184−6193

adsorbents. Furthermore, such Al-rich zeolites can stabilize bare divalent cations such as Cu^{2+}, Fe^{2+}, and Ni^{2+} for several specific catalytic applications.[9,10] However, they are not always desirable since water molecules can attack hydrophilic Al sites, making them not hydrothermally stable to utilize in a certain industrial applications.[11,12] In high silica aluminosilicate zeolites, the substituting amounts directly correlate with the acid amounts in zeolites (in their proton-form). As is well documented, the location of Al can have dramatic influences on the catalytic performances of zeolites.[13−16] For example, only Al in small pores of zeolites can create acid sites that are able to catalyze the carbonylation of methanol.[13] In addition to the framework topology, the Al contents and locations in the zeolite frameworks are therefore the key parameter of zeolites, and their precise controls are of vital importance to achieve zeolites with desired properties.[1,9]

Recent advances in characterization and computational techniques have enabled us to quantitatively analyze the Al distributions in zeolites,[9,17−19] and consequently the relations between Al distributions and properties, particularly, catalytic behaviors, of zeolites have been established for some specified cases of study.[9,13−16] It is well-known, however, that many properties of zeolites can be influenced not only by the Al contents and distributions, but also by several other characteristics such as crystal morphology and defect sites. As a result, direct experimental correlation between Al distributions and properties of synthesized zeolites becomes more complicated and, therefore, requires great attentions as the changes in properties that seem to be arisen from Al distributions can be also affected by other factors.

The energetics of zeolites, on the other hand, are intrinsic properties of zeolite with the given topology and composition, which have been studied intensively by calorimetry.[20] These energetic properties of zeolites, particularly expressed as framework (lattice) energies versus molar volumes or framework densities of zeolites, have been used to predict the thermodynamically feasible zeolites and also can provide the energetic clues to the formation pathways and phase equilibria of zeolites.[6−8,20,21] Although the effects of the zeolite topologies and Al contents on the energetics of zeolites have been reported experimentally,[20,22] the large-scale, systematic establishments of such relations for all zeolite topologies with a wide range of Si/Al ratios and various Al distributions experimentally are impossible because the available Si/Al ratios of existing aluminosilicate zeolites are generally limited to a certain range depending on their topologies. For instance, the aluminosilicate zeolite with LTA topology is typically synthesized with a Si/Al ratio of 1, while MFI-type zeolite has higher Si/Al ratios up to ∞ (i.e., pure silica). Moreover, many zeolites have never existed in aluminosilicate compositions, although considerable synthetic efforts have been devoted for expansion of their realizable compositions. Therefore, the full experimental data set for the energy landscape of aluminosilicate zeolites is far from complete.

On the contrary, computational methods can provide possible access to all zeolite topologies including hypothetical ones with any compositions, Al distributions, and types of counterions. Density functional theory (DFT) calculations with either periodic boundary conditions or cluster models have revealed the relations between framework energies versus locations and contents of substituting T atoms (e.g., Al, Ge, and Sn) and subsequently suggested the preferred location and type of substitutes.[23−26] Due to their expensive computational costs, however, these computations have focused on the limited ranges of compositions and the limited numbers of topologies; consequently, the full energy landscapes resulted from all topologies, compositions, and distributions of substitutes have never been explored. Unlike DFT-based methods, a lattice-energy minimization technique using reliable, analytical potentials (or force fields) has successfully been employed to predict structures and properties of zeolites.[27] The energy minimization using potentials that were developed exclusively for zeolites, for example, the Sanders−Leslie−Catlow (SLC) interatomic potential optimized for (alumino)silicate zeolites,[28,29] became a de facto standard for constructing the database of zeolite topologies.[7,8,29−31] Such potentials allow us to evaluate zeolite structures and properties in larger scales because of their reliable accuracy and relatively low computational cost.

We describe herein the systematic computational evaluation of the energetics of aluminosilicate zeolites with 209 existing framework topologies having different Al contents (Si/Al = 1, 3, 7, 15, 31, and ∞) and distributions using the SLC potential assisted by a Monte Carlo sampling. For all topologies, the substituting Al atoms are located randomly or placed at specific crystallographic T sites. To the best of our knowledge, this comprehensive data set for the energetics of aluminosilicate zeolites is presented for the first time. The energetics of aluminosilicate zeolites depend not only on the framework topologies, but also on the Al contents and locations, implying that a given framework topology of zeolites has favorable Al contents and sites inherently.

METHODS

As of the starting of our computations, there were 218 zeolite framework types catalogued by IZA. By excluding 9 interrupted framework topologies and RWY (an unusual topology existing only as chalcogenides) but including BEB (a polymorph B of zeolite beta), 209 topologies were selected for our computations.[32] Coordinates of each topology (in pure silica compositions) were obtained as CIF files downloaded from IZA's database.[4] The energy minimizations were performed on the GULP program[33] with the SLC potential under the constant pressure condition. The framework energies reported here were calculated relative to α-quartz. The computational cells were converted to a $P1$ space group symmetry to allow the atomic positions and other crystallographic parameters to be altered during the molecular mechanics optimization. For pure silica compositions, the computational cells were in a unit-cell size, while the super cells were used for aluminosilicate counterparts.

The super cells were created by expanding each unit cell until the number of T atoms reached the following conditions: (i) to increase the randomness of Al distribution, the number of T atoms was more than 100; and (ii) to achieve the targeted substituting contents of Al, the number of T atoms was the multiples of (Si + Al)/Al molar ratios. Because the required computational resources are increased as the number of T atoms in the super cells increases, we tried to avoid unnecessary expansion of the unit cells by choosing the targeted substituting contents of Al with the (Si + Al)/Al molar ratios being the power of 2 (i.e., 2, 4, 8, 16, and 32), resulting in the Si/Al of 1, 3, 7, 15, and 31, respectively. In extreme cases in which the number of T atoms in the unit cells is odd numbers (i.e., OSO and VET topologies), the super cells were 32 times larger than their unit cells for achieving the Si/Al of 31.

After creating the super cells, the initial aluminosilicate structures were generated with different Si/Al ratios by substituting SiO_4 tetrahedra in the pure silica polymorphs with AlO_4 randomly while avoiding Al−O−Al bonding to obey Löwenstein's rule[34] until the desired Si/Al ratios were achieved. For random substitution, the Mersenne Twister algorithm was used to generate the pseudorandom

DOI: 10.1021/jacs.6b01341
J. Am. Chem. Soc. 2016, 138, 6184−6193

numbers.[35] When the Si/Al ratios were 3, 7, 15, and 31, initial structures with 10 different Al configurations/distributions were constructed for each Si/Al ratio. For the Si/Al of 1, however, only two possible configurations were created. Note that many zeolite topologies cannot yield the structures with the Si/Al of 1 because they contain odd-numbered rings and thus cannot avoid the formation of Al−O−Al bonds. As a result, only 99 topologies having only even-numbered rings were computed for the Si/Al of 1. To study the influences of Al distribution (random versus nonrandom) on the framework energy, in addition, Si at specific crystallographic T sites were substituted by Al to reach the targeted Si/Al ratios.

After Al substitution, one of four O atoms directly connected to Al was randomly selected and protonated. The initial positions of protons were decided according to the following vector equation:

$$\mathbf{h} - \mathbf{o} = \frac{(\mathbf{o} - \mathbf{t}_1) + (\mathbf{o} - \mathbf{t}_2)}{|(\mathbf{o} - \mathbf{t}_1) + (\mathbf{o} - \mathbf{t}_2)|} \times 0.9485 \quad (1)$$

where $\mathbf{h}$ is the positional vector of proton, $\mathbf{o}$ is the positional vector of the protonated O atom, $\mathbf{t}_1$ and $\mathbf{t}_2$ are the positional vectors of the neighboring T atoms, and 0.9485 is the initial O−H bond length (in angstrom).[29] If $\mathbf{t}_1-\mathbf{o}$ was parallel to $\mathbf{t}_2-\mathbf{o}$, the direction of $\mathbf{h}-\mathbf{o}$ was determined randomly. For each Al configuration, 5 combinations of proton locations were decided. The most energetically favorable proton configuration was selected from the converged optimizations for each Al configuration.

RESULTS AND DISCUSSION

In zeolite chemistry, in addition to aluminosilicate zeolites, aluminophosphate is the most conventional composition for zeolite-like materials. Throughout this article, therefore, the conventional zeolite topology is referred to as the topologies that are really present as zeolites or zeolite-like materials in pure silica, aluminosilicate, aluminophosphate, or silicoaluminophosphate compositions, akin to the previous report.[31] In contrast, the topologies that have never existed in one of the above-mentioned compositions are called unconventional topology.[31] In such unconventional zeolites, the substitution of unconventional T atoms (e.g., Be, Zn, B, and Ge) possessing different T−O bond lengths, T−O−T bond angles, and/or charges can inherently stabilize some structural building units, thereby directing the formation of zeolites with unusual topologies.[36] As a result, the energetics of aluminosilicate zeolites with unconventional topologies may differ from those of conventional ones.

A total of 43 409 initial structures with different topologies, Si/Al ratios, Al locations, and proton configurations were generated and optimized. Average T−O bond lengths, and T−O−T and O−T−O bond angles summarized in Tables S1 and S2 in the Supporting Information (SI), respectively, were within the reasonable ranges of zeolites described in the literatures.[29,31,37] The plot of framework energy with respect to α-quartz versus framework density for all the optimized structures with the most energetically favorable configuration of protons is shown in Figure 1a. Shifts of the data points toward lower densities were clearly observed upon the Al substitutions, suggesting the expansion of framework volumes (vide infra). The frameworks energies increased as the substituting contents of Al were increased. This is because Al is a next lighter element than Si; therefore, the framework energies with respect to α-quartz of aluminosilicate zeolites become higher than those of the pure silica counterparts. Consequently, the direct comparison of the framework energies between zeolites with different contents of Al requires a reasonable way to normalize the computed energies. Akin to

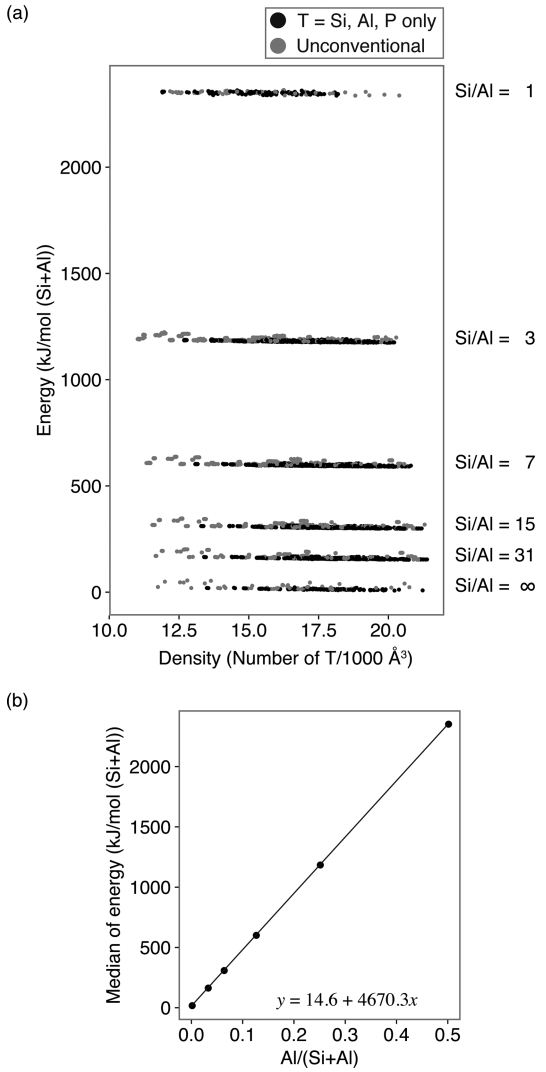

Figure 1. (a) Framework energy (kJ per mole of T atoms) with respect to α-quartz versus framework density (numbers of T atoms per 1000 Å^3) for all topologies and Al configurations with different Si/Al ratios. Black and gray symbols represent conventional and unconventional topologies, respectively. (b) Relation between medians of framework energy and molar fractions of Al.

the previous reports experimentally showing the linear correlations between the enthalpies of formation from oxides of aluminosilicate zeolites and the substituting contents of Al,[20,22] in our computations, a relation between framework energies and Al/(Si+Al) molar fractions was observed as shown in Figure 1b. The Pearson product-moment correlation coefficient was 1, within the numerical error, indicating the clear linear relationship. For comparison, the relative framework energy of the optimized structure at a given Si/Al ratio (E_{relative}) is offset by the median of all framework energies obtained at the same composition ($E_{\text{median-of-a-given-Si/Al}}$), as expressed below:

$$E_{\text{relative}} = E_{\text{computed}} - E_{\text{median-of-a-given-Si/Al}} + E_{\text{median-of-Si/Al=}\infty} \quad (2)$$

where E_{computed} is the computed framework energy with respect to α-quartz and $E_{\text{median-of-Si/Al=}\infty}$ is the median of all framework energies obtained for the pure silica composition.

DOI: 10.1021/jacs.6b01341
J. Am. Chem. Soc. 2016, 138, 6184−6193

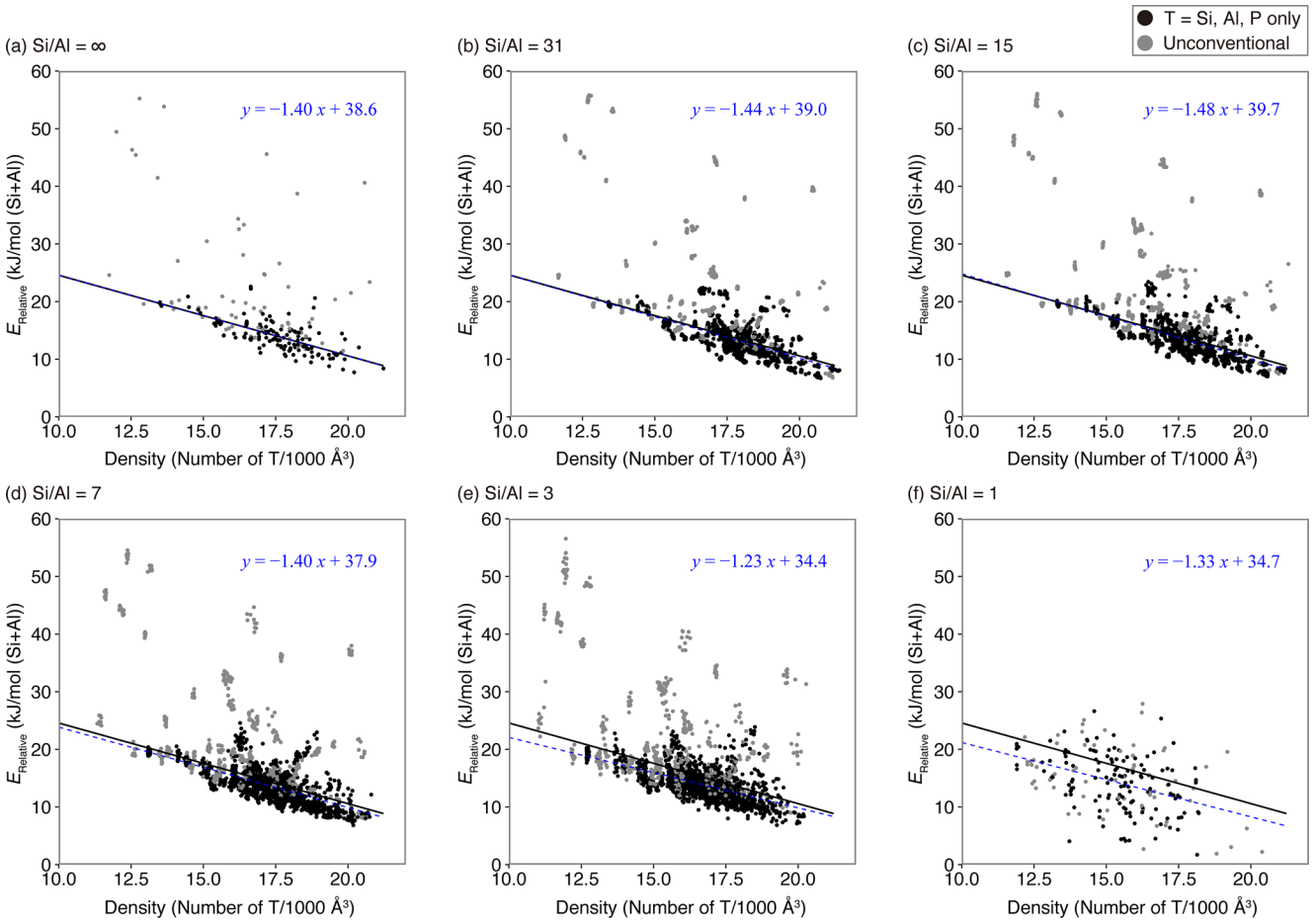

Figure 2. Relative framework energy, $E_{Relative}$ (kJ per mole of T atoms), versus framework density (numbers of T atoms per 1000 Å^3) for all topologies and Al configurations with Si/Al of (a) ∞ (i.e., pure silica), (b) 31, (c) 15, (d) 7, (e) 3, and (f) 1. Black and gray symbols represent conventional and unconventional topologies, respectively. The solid line in each plot is a regression line derived from conventional topologies with Si/Al = ∞, while the dashed line is fitted to the data set of conventional topologies for each Si/Al ratio. The fitting equations for each regression line are shown in each plot.

Figure 2 shows the relations between the relative (offset) framework energies versus framework densities at different Si/Al ratios. The solid line in each plot is a regression line derived from conventional topologies with the pure silica composition whereas the dashed line is fitted to all data points of conventional zeolites for each Si/Al ratio (also see Figure S1 in the SI for the combined plots of all the regression lines). The resulting fitting parameters for each linear regression line are shown in Figure 2. For Si/Al = ∞ (Figure 2a), the computed values well reproduced the results reported previously[8,31,38] but were updated with newly discovered structures, showing that the framework energies decreased as the framework densities increased. The framework energies with respect to α-quartz of conventional zeolites at Si/Al of ∞ ranged from 7.73 to 22.6 kJ/mol, depending on the framework densities.

As shown in Figure 3a, upon the substitution of Al for Si the framework densities of the optimized structures decreased, indicating the increases in framework volumes, because the average bond length of Al−O is longer than that of Si−O (also see Table S1 in the SI). Similar to the pure silica composition, relations between relative framework energies and framework densities were observed for aluminosilicate zeolites (Figure 2b−f). However, the data points became more scattering as the substituting contents of Al were increased (i.e., the decreased

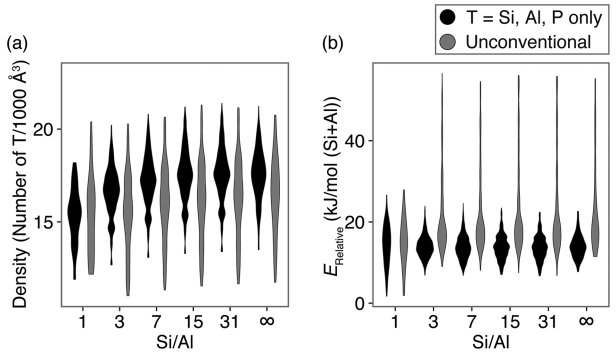

Figure 3. Violin plots of (a) framework density and (b) relative framework energy versus Si/Al ratio. Black and gray symbols represent conventional and unconventional topologies, respectively.

Si/Al ratios), suggesting the effects of Al locations on the energetics of aluminosilicate zeolites.

Figure 3b compares the relative framework energies for zeolites with different Al contents, indicating similar energetics of (alumino)silicate zeolites over a complete range of Si/Al ratios. As shown in Figure S1 in the SI, however, the regression lines derived from all conventional topologies shifted toward lower relative framework energies as the substituting contents

DOI: 10.1021/jacs.6b01341
J. Am. Chem. Soc. 2016, 138, 6184−6193

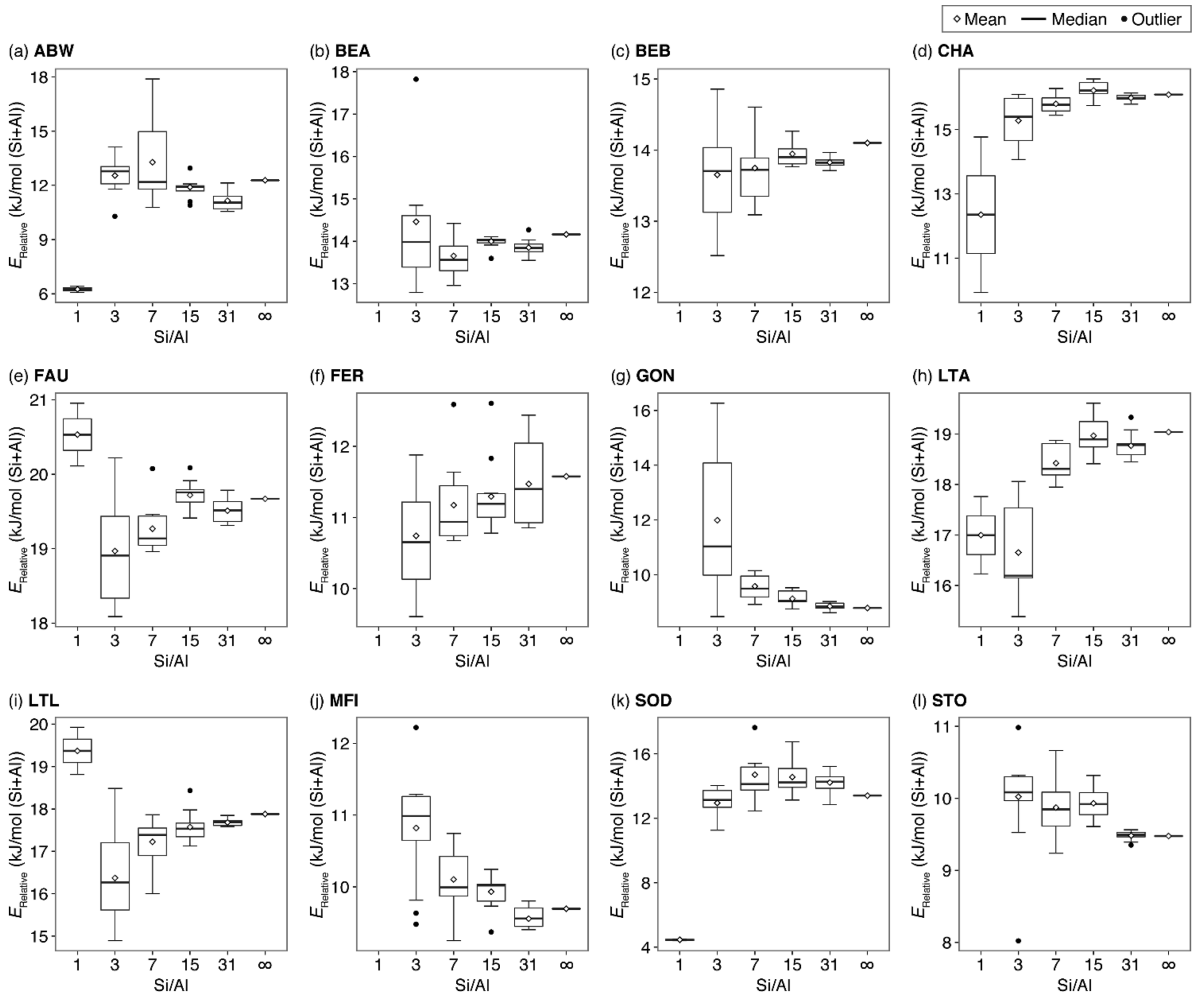

Figure 4. Box plots of relative framework energy versus Si/Al ratio for selected topologies. The top and the bottom of the box are 75 and 25 percentiles, respectively. The bold bar inside the box indicates 50 percentile (i.e., median), while the open diamond indicates mean. The upper and the lower are the most extreme data points within 1.5 times of the interquartile range. Outliers, the data points outside of this range, are expressed as closed circles.

of Al were increased, likely reflecting the increase in relative thermodynamic stability of zeolites upon the Al substitutions.

If the relative framework energy is unique to the zeolite topology but independent of the chemical composition, the slopes of the regression lines for the Si/Al ratios of 3, 7, 15, and 31 have to be identical because these 4 subsets of data were obtained from the similar computations. However, the fitted regression lines were not parallel, suggesting that the energetic effects of the Al substitutions depend on both zeolite topologies and chemical compositions. For detailed investigation, distributions of relative framework energies at different Si/Al ratios for all 209 topologies are plotted in Figure S2 in the SI with those of 12 representative topologies known to be synthesized as aluminosilicate zeolites with Si/Al ratios covering all ranges of compositions shown in Figure 4. Based on the structural features of zeolites, zeolite topologies can be grouped into (i) those containing only even-numbered rings and (ii) those having both even- and odd-numbered rings. Therefore, we have selected six topologies constructed from only even-rings (ABW, CHA, FAU, LTA, LTL, and SOD) and six topologies constructed from both even- and odd-rings (BEA, BEB, FER, GON, MFI, and STO) for detailed discussion (Figure 4).

The distributions revealed that even if the topology and the Al content were identical, the computed energy had a certain distribution. This distribution seems to be not too significant to prevent a particular Al and proton configuration. As for MFI topology with Si/Al of 31, the difference between the least stable Al configuration and the most energetically preferable one was only 0.40 kJ/mol, consistent with a periodic DFT calculation on high silica H-ZSM-5, a proton-form MFI-type zeolite,[39] but with increasing Al contents, the energy difference became larger as 0.9 kJ/mol (Si/Al = 15), 1.5 kJ/mol (Si/Al = 7), and 2.7 kJ/mol (Si/Al = 3). The difference in energy distributions was dependent on zeolite topologies and chemical compositions, again implying that the thermodynamic stability and the existence of preferential Al sites rely on both topologies and compositions.

In zeolite synthesis, cations, either inorganic or organic, are always added to the synthesis mixtures to direct the formation of a particular zeolite under a given synthesis condition. Comparisons between the computed results and the typically existing zeolites can therefore give some physical understanding relevant to the "equilibrium" zeolite products and may provide some energetic clues related to the zeolite formation. It is noteworthy that in our calculations a proton is the counterion, instead of alkali cations or organic structure-directing agents

DOI: 10.1021/jacs.6b01341
J. Am. Chem. Soc. 2016, 138, 6184−6193

(OSDAs) typically used for the synthesis of zeolites. Therefore, the computed energy results are thought to be arisen intrinsically from the structures of aluminosilicate zeolites.

ABW is one of the topologies constructed solely from even-numbered rings, possible to realize Si/Al = 1 without violating Löwenstein's rule.[34] As shown in Figure 4a, the energy results clearly suggested that ABW with Si/Al of 1 is the most thermodynamically stable, which is consistent with the experimental observation found in zeolite Li-A, a type material of ABW,[4] having the composition of Si/Al = 1,[40] although they contain different counterions. CHA is another topology consisting of even rings only. Its most energetically favorable composition is predicted to be Si/Al of 1 (Figure 4d). The synthetic CHA-type zeolites can have a wide range of compositions from Si/Al of ∼2 to pure silica, depending on synthesis conditions and cations used,[41,42] while chabazite minerals, the natural zeolite of CHA, possess Si/Al ratios of 1.4−4, depending on types of counterions.[43,44] These can imply that natural and some of synthetic CHA-type zeolites are close to the equilibrium zeolite product, while the synthetic zeolites, particularly those synthesized by using OSDAs, are stabilized alternatively. The computed average energy of SOD at Si/Al of 1 is exceptionally lower than other compositions (Figure 4k), clearly reflecting its naturally occurring and conventionally synthesized forms at Si/Al of 1.[42,44] It should be mentioned that SOD-type zeolites can be synthesized at higher Si/Al ratios up to ∞ (i.e., pure silica) through unconventional synthetic routes, for example, nonaqueous, solvothermal synthesis using OSDAs[45] and topotactic conversion of a layered silicate precursor.[46]

Not all topologies having only even rings favor Si/Al of 1; FAU, LTA, and LTL are discussed here as examples (Figures 4e, h, and i, respectively). One of the representative FAU-type zeolites is Linde Y zeolite, of which Si/Al ratios are 1.5−3, with the most typical ratio being ∼2.5,[47] close to the most energetically favorable composition of 3 (Figure 4e). By varying synthesis parameters, the Si/Al ratios of FAU-type zeolites can be lowered to 1 found in low-silica X (LSX) zeolite when sodium and potassium cooperatively work as inorganic structure-directing agents,[48] and also increased to about 4 by using OSDAs.[42] The higher energies of FAU-type zeolites with Si/Al of 1 and >3 would reflect their unconventional and/or narrow synthetic conditions. LTA is one of the most widely used zeolites with Si/Al of 1 typically synthesized with sodium as the counterion, but its feasible compositions have been broadened by use of OSDAs and fluoride media, which is likely inapplicable for the present calculation. Our result shown in Figure 4h favored Si/Al ratios of 3 and 1, respectively, which is agreed with the recent HOU-2 zeolite (Si/Al = 2.1)[49] and the typical zeolite A (Si/Al = 1),[50] synthesized without using OSDAs. As depicted in Figure 4i, the most energetically favorable composition of LTL was Si/Al of 3, which is identical to the molar ratio of Linde L zeolite (a type material of LTL).[4,51] Although both CHA and LTL topologies are constructed from the double 6-ring (*d6r*) structural building unit, their most energetically favorable compositions were different (see Figure 4d and i), suggesting that the energetics of aluminosilicate zeolites are not simply correlated to basic structural building units. Rather, more complex effects involving the ways that building units assemble, causing different bond lengths and angles, have to be considered.

In contrast to topologies that contain only even rings, topologies having odd rings are generally present as high silica zeolites as the adjoining aluminate tetrahedra (i.e., Al−O−Al linkages) are energetically unstable due to the unfavorable interactions arising from the cluster of negative charges. It was suggested that if two aluminate tetrahedra are adjacent, at least one of them must have a coordination number larger than four (i.e., five or six).[34] Five-ring (*5r*) is the most typical odd-ring found in zeolite topologies whereas there-, seven-, nine-, and 11-ring rarely exist.[6,52] As a result, there is an established empirical rule that high silica zeolites tend to have *5r* (vice versa).[45]

As the representative zeolites of *5r*-containing topologies, zeolite beta, possessing the intergrown structure of BEA and BEB,[53] and ZSM-5 (a type material of MFI)[4,54] were two first synthetic, high silica zeolites synthesized using OSDAs. As shown in Figure 4b and c, both BEA and BEB did not show significant differences of average energies (within variation of 1 kJ/mol). Zeolite beta is another example of zeolites that can be obtained in a wide range of Si/Al ratios (3 to ∞). In the absence of OSDAs, zeolite beta synthesized by a seed-assisted method can have Si/Al ratios as low as 4.5,[55] while its mineral counterpart, tschernichite,[44] has Si/Al of ca. 3.[56] For MFI topology, the compositions of Si/Al = 31 and pure silica seemed to be energetically favorable than others (Figure 4j). MFI-type zeolites are typically synthesized under relatively high Si/Al ratios,[57] and its pure silica polymorph, silicalite-1, can also be realized.[58] Note that MFI-type zeolite with a relatively low Si/Al ratio of 9.3 can be obtained by seed-assisted, OSDA-free synthesis.[59]

STO- and GON-type zeolites are examples of zeolites that always need OSDAs for their syntheses and do not have naturally occurring minerals.[4] They showed the lowest average energies at Si/Al of ∞ or 31 (see Figure 4g and l), consistent with the experimental observations.[60,61] FER possessed the most energetically favorable composition of Si/Al = 3 (Figure 4f), slightly lower than the compositions found in its natural mineral, ferrierite (Si/Al = 5).[44] Direct synthesis of FER-type zeolites (nonseed and OSDA-free) yields zeolites with Si/Al of 6−12, depending on alkali cations used.[62]

As summarized in Figure S3 in the SI, numbers of topologies that possess the minimum of the average relative framework energy at Si/Al ratios of 1, 3, 7, 15, 31, and ∞ are 59, 61, 15, 13, 48, and 13 topologies, respectively. The relations between framework topologies, chemical compositions, and thermodynamic stability are sometimes explained on a basis of ring size distribution.[45,52] The topologies that have the lowest of the average energy at Si/Al ≥ 7 are dominated by zeolites containing *5r*, while the topologies stable at Si/Al ≤ 3 are dominated by those constructed solely from even rings. For topologies favoring Si/Al of 3, the average ring size distribution of four-ring (*4r*) (28%) is higher than that of *5r* (17%). At higher Si/Al ratios, the existence of *5r* may stabilize the frameworks as the previous study suggested that *5r*- and *6r*-silica are more stable than *4r*.[63] Substitution of Al for Si may relax the unfavorable bond lengths and angles of *4r* in the pure silica framework, thereby yielding aluminosilicates with lower Si/Al ratios. It is, however, difficult to simply explain the origins of this dependency based on basic structural features such as ring size distribution alone because the energetics of aluminosilicate zeolites seem very complicated, as discussed above.

In the typical tetrahedral frameworks, Si−O and Al−O bond lengths are ca. 1.61 and 1.73 Å, respectively, with O−T−O bond angles close to the tetrahedral angle (109.47°).[64] In the

DOI: 10.1021/jacs.6b01341
J. Am. Chem. Soc. 2016, 138, 6184−6193

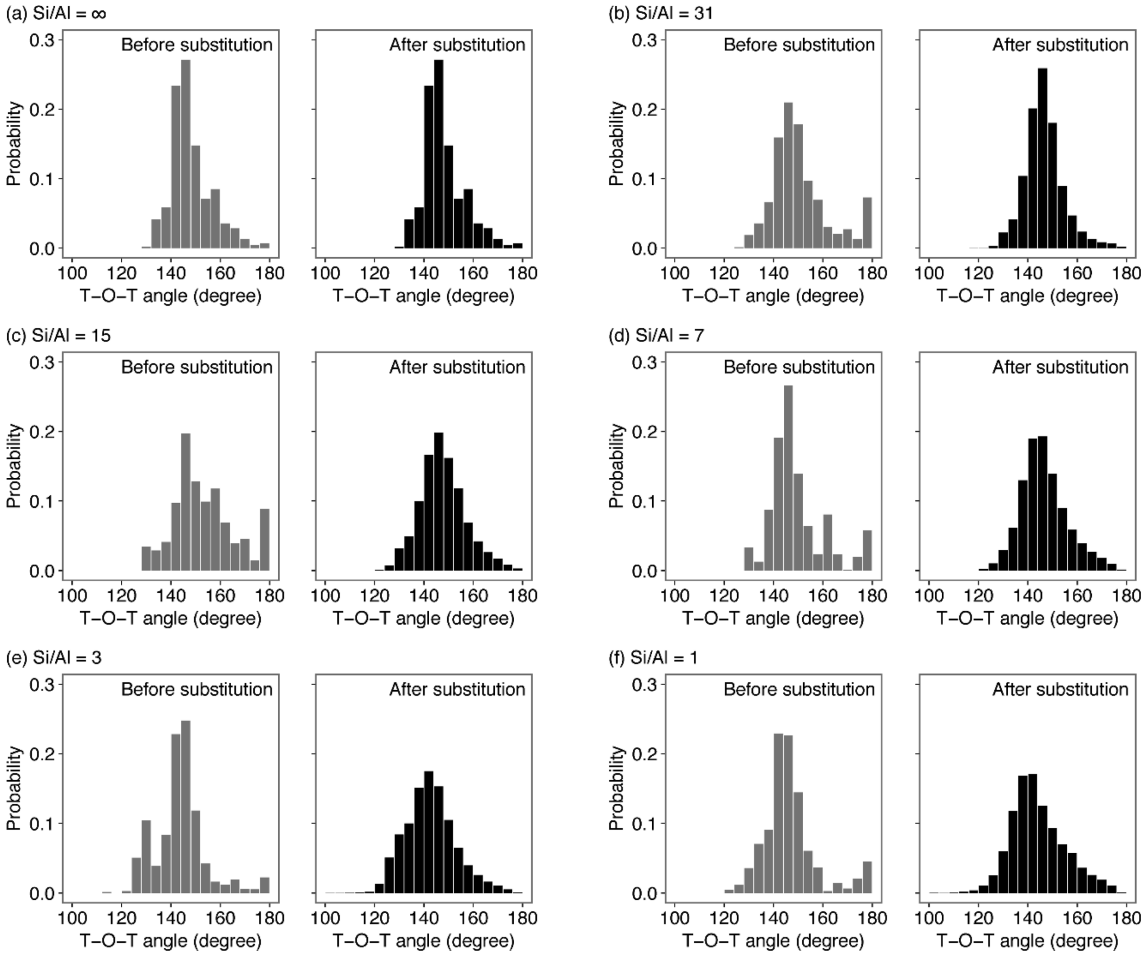

Figure 5. T–O–T angle distributions for optimized pure silica models (i.e., before Al substitution; gray) and corresponding optimized models at the most energetically favorable aluminosilicate compositions (i.e., after Al substitution; black) of topologies that energetically favor Si/Al of (a) ∞, (b) 31, (c), 15, (d) 7, (e) 3, and (f) 1.

frameworks without constraints such as α-quartz, T–O–T bond angles were found to be in a narrow range close to 145°.[65] Due to the difference in bond distances between Si–O and Al–O, the distortion of tetrahedral primary units stemming from the substitution of Al for Si should be relaxed by altering the T–O–T angles. A previous theoretical study proposed that $AlO_{4/2}$ tetrahedron is stabilized at the sites with relatively smaller T–O–T angles.[66] For existing zeolites, T–O–T angles can be varied, while maintaining the regular tetrahedral geometry, reflecting a "flexible window" over a range of framework densities.[67] Such flexibility was also found experimentally in synthetic, pure silica zeolites as their Si–O–Si angles range from 133.6 to 180°, with a mode value of 148° and a mean value of 154 ± 9°, while keeping their Si–O bond lengths and O–Si–O angles close to the typical values.[37]

To rationalize the underlying relations between framework topologies and chemical compositions based on the basic structural descriptor, the probability distributions of T–O–T angles were calculated and are summarized in Figure 5. We categorized 209 topologies into 6 groups according to their most energetically favorable Si/Al ratios. In Figure 5, the probability distributions of their T–O–T angles for *pure silica models* are shown as gray histograms, in comparison with their *aluminosilicate models* at the most favorable Si/Al ratio displayed in black. The topologies having the lowest average energies at Si/Al = ∞ such as GON were unlikely to have T–O–T angles less than 130° (Figure 5a), consistent with the previous experimental analysis.[37] As shown in Figure 5b (gray histograms), a similar trend was observed in the pure silica model for the topologies favoring Si/Al of 31 (e.g., MFI). Considering their pure silica models (gray histograms in Figure 5b–f), the probability of the smaller T–O–T angles increased with decreasing favorable Si/Al ratios, probably suggesting the less stability of their pure silica polymorphs due to the unfavorable T–O–T angles. In addition, it was observed in the pure silica models (see gray histograms) that the fractions of unusual, large T–O–T angles close to 180° were quite small for the topologies preferring the pure silica composition (Figure 5a) but somewhat higher for the rest of topologies favoring aluminosilicate compositions (Figure 5b–f).

We surmise that the substitution of Al at the most energetically favorable aluminosilicate compositions should relax the framework strains and distortions causing such unusual T–O–T angles observed in the pure silica models. In addition, the T–O–T angles of the optimized structures at the most stable composition should be close the ideal value for the unstrained Si–O–Si (i.e., 145°). For the topologies with the favor Si/Al of 31, interestingly, their optimized aluminosilicate structures did not show extremely large T–O–T angles (Figure 5b, black histograms). Clearer changes in the T–O–T angle distributions were observed in the topologies favoring lower Si/Al ratios (Figure 5c–f). The

DOI: 10.1021/jacs.6b01341
J. Am. Chem. Soc. 2016, 138, 6184–6193

probability distributions of T−O−T angles of the aluminosilicate models at the most favorable Si/Al ratios displayed Gaussian-like distributions centered close to 145°, indicating that the optimized structures at the most energetically favorable compositions should possess as few as possible the strained T−O−T linkages.

As the positions of Al can have massive effects on the properties of zeolites, one of the ultimate goals in zeolite chemistry is to develop the rational synthetic methods that can allow for the specific placement of Al at the designated crystallographic T sites in the zeolite frameworks.[1,13] From the viewpoint of symmetry, in addition, zeolites with the specific Al distribution are conceived to be energetically more stable than those with random distribution. So far, there have been several investigations attempting to alter the Al distributions by varying synthesis parameters such as raw materials of silica and alumina, types of OSDAs and alkali cations, and temperature.[15,16,68,69] Although the Al distributions can be narrowed to a certain degree, the synthesis that results in the specific crystallographic site for Al is still far from success. It is therefore of great scientific interest to examine whether there are any energetic barriers that prevent the placement of Al at the specific crystallographic site.

We screened several zeolite topologies that are crystallographically possible to yield aluminosilicate structures with the specific crystallographic T site for Al without forming Al−O−Al linkages. Four topologies, namely, BEA, CON, MFI, and MWW, that can realize specific Al distributions using different crystallographic T sites at the same Si/Al ratios were selected as examples. It is noteworthy that the effects of Al distributions in these topologies on the catalytic performances have been reported recently.[10,16,69−71] Figure 6 shows the computed relative framework energies of zeolites with specific Al sites in comparison with the energy distributions observed for the Al random distributions having identical Si/Al ratios. Crystal structures with labeled T sites of BEA, CON, MFI, and MWW are illustrated in Figures S4−S7 in the SI, respectively. Note that the T sites are labeled according to the CIF files taken from the IZA's database.[4] Substitutions of Al into T8 and T9 sites of BEA created the aluminosilicate structures with Si/Al of 15 whereas substitutions into T3, T4, T5, T6, and T7 sites yielded Si/Al of 7. Note that substitutions of Al into all T1 and T2 sites were not possible as they resulted in Al−O−Al linkages. As shown in Figure 6a, the relative framework energy of BEA with Al at the T8 site was lower than those with Al at the T9 site and random Al distribution, suggesting that T8 is the most energetic favorable site for BEA with Si/Al of 15. For BEA with Si/Al of 7, all structures with specific Al sites were energetically more stable than that with random distribution, with the lowest energy found at the T6 site (Figure 6b). As reported recently, Al-rich zeolite beta (the intergrowth of BEA and BEB) synthesized without using OSDAs can stabilized Fe^{2+} for NO adsorption.[10] Detailed analyses later indicated that in such Al-rich zeolite beta most of the Al pairs were located at the β-type ion-exchange site.[70] Interestingly, as illustrated in Figure 7, the T6 and T8 sites, the most energetically favorable site for BEA with Si/Al of 7 and 15, respectively, are a part of the β-site, suggesting our computational results may somewhat reflect the experimentally observed Al sites in the OSDA-free synthesized, Al-rich zeolite beta.[55,70]

CON and MFI topologies also showed that the structures with specific Al sites were energetically more stable than that with random distribution. Among several T sites, the T2 site of CON (at Si/Al = 6) and the T3 site of MFI (at Si/Al = 11) were found to be the most energetically favorable (see Figure 6c and d). In contrast to BEA, CON, and MFI, the structures

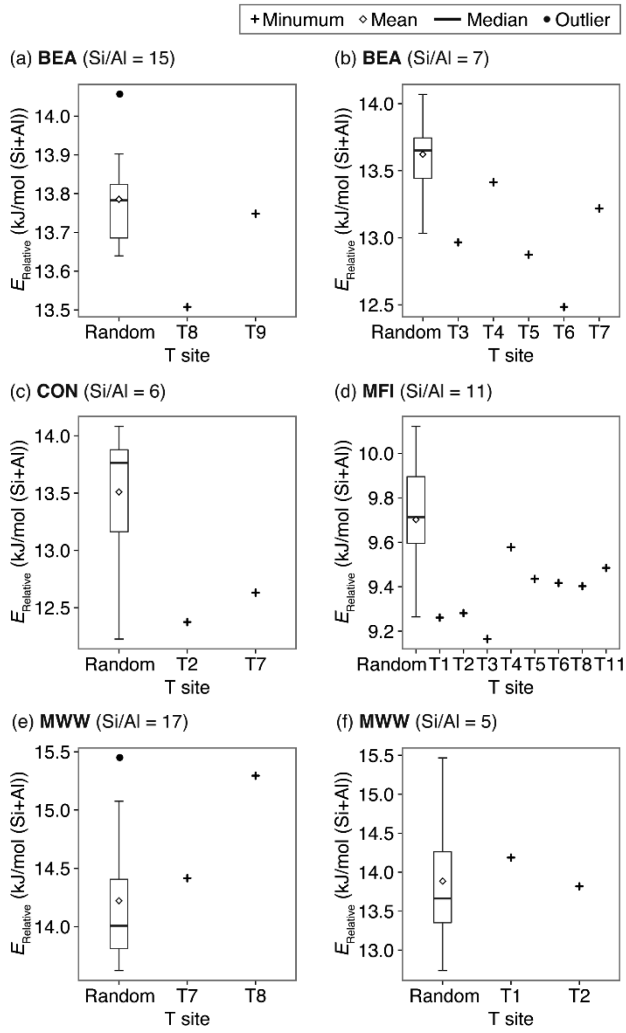

Figure 6. Relative framework energy of the optimized structures with specific Al locations at different T sites, in comparison with random Al distributions.

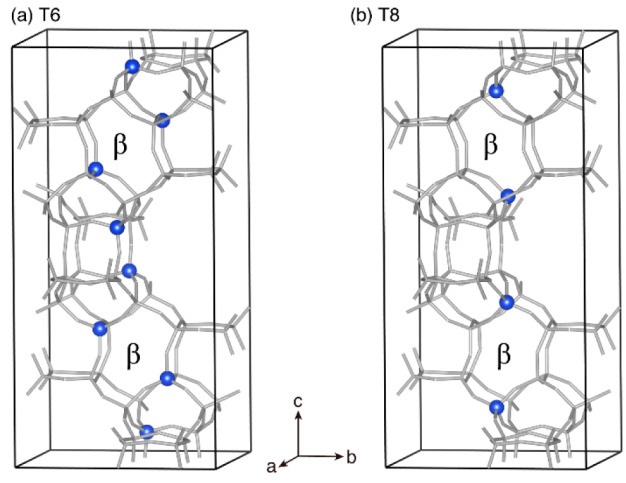

Figure 7. Crystal structure of BEA topology displaying the β-type, six-ring ion-exchange site with the highlighted (atoms in blue) (a) T6 and (b) T8 sites.

DOI: 10.1021/jacs.6b01341
J. Am. Chem. Soc. 2016, 138, 6184−6193

with random Al distributions seemed to be energetically more stable than or similar to those with specific Al locations for MWW topology with Si/Al of 5 and 17 (see Figure 6e and f).

CONCLUSIONS

The energetics of aluminosilicate zeolites possessing comprehensive ranges of possible structural configurations were evaluated computationally and presented here for the first time. A total of 43 409 (alumino)silicate zeolite structures with 209 different topologies, Si/Al ratios ranging from 1 to ∞, different Al locations (random versus specific), and proton configurations were generated with the aid of the Monte Carlo method and then optimized by the lattice-energy minimization technique. The linear relationships between framework energies and framework densities were found to be similar, but not exactly identical, to the previous reports on their pure silica counterparts. Comparison of the relative framework energies of each topology with different Al contents indicated that the relative thermodynamic stability of zeolites depends not only on the framework topologies, but also on the substituting contents of Al. In addition, it was revealed that the framework structures of zeolites at the most energetically favorable Al contents have the T−O−T bond angles close to the typical value for the unstrained Si−O−Si linkages, reflecting the intrinsic influence of structural features of each topologies. For particular framework topologies with the identical Al contents, the aluminosilicate zeolite with Al at a specific location was energetically more stable than those with random distributions. Within the intrinsically narrow range of framework energy, the contents and the locations of Al in the zeolite frameworks seem to have a certain preference that is probably related to the range of chemical compositions, the Al distributions, and consequently the physicochemical properties of feasible aluminosilicate zeolites.

Although in our computations the anionic aluminosilicate zeolites were treated with the discrete values of Si/Al and the protons as counterions, the results coincided well with the structural knowledge obtained experimentally. In general, the formation of zeolites has been thought to be controlled kinetically; however, many framework topologies, of which the computed results even in the proton-forms agreed well with the experimental observations, can presumably be present as aluminosilicate zeolites with their most energetically favorable configurations (in terms of Al contents and locations). More intense computations are required to grasp the whole energy landscape of aluminosilicate zeolites with continuous variation of Si/Al ratios and different types of counterions such as alkali cations and organic structure-directing agents that would further provide the energetic clues to the formation pathways of zeolites, which may appear in the future studies. In addition, similar calculations on other substituting atoms such as B and Ga, which needs alternative potentials, merit future investigation. Considering the large set of data achieved here, chemometrics and related statistic tools should be applied to interpret the data and to further correlate them with the structural properties of zeolites.[72]

ASSOCIATED CONTENT

Supporting Information

The Supporting Information is available free of charge on the ACS Publications website at DOI: 10.1021/jacs.6b01341.

Mean T−O bond lengths and T−O−T angles, combined plot of the regression lines, plots of relative framework energies versus Si/Al ratios for all topologies, plot of number of topologies having the minimum mean energy at each Si/Al ratio, and crystal structures of some selected frameworks (PDF)

AUTHOR INFORMATION

Corresponding Authors

*watcha@chemsys.t.u-tokyo.ac.jp
*okubo@chemsys.t.u-tokyo.ac.jp

Notes

The authors declare no competing financial interest.

ACKNOWLEDGMENTS

This work was supported in part by Grant-in-Aids for Scientific Research (A) (Grant Number: 26249118) and for Research Activity Start-up (Grant Number: 26889022) by the Japan Society for the Promotion of Science (JSPS). K.M. thanks the Program for Leading Graduate Schools, "Global Leader Program for Social Design and Management (GSDM)," by the Ministry of Education, Culture, Sports, Science and Technology (MEXT) for financial support. Computations were partly performed using the computers at the Research Center for Computational Science, Okazaki, Japan.

REFERENCES

(1) Davis, M. E. *Chem. Mater.* **2014**, *26*, 239−245.
(2) Snyder, M. A.; Tsapatsis, M. *Angew. Chem., Int. Ed.* **2007**, *46*, 7560−7573.
(3) Moliner, M.; Martínez, C.; Corma, A. *Chem. Mater.* **2014**, *26*, 246−258.
(4) Database of Zeolite Structures, http://www.iza-structure.org/databases/.
(5) Atlas of Prospective Zeolite Structures, http://www.hypotheticalzeolites.net/.
(6) Li, Y.; Yu, J. *Chem. Rev.* **2014**, *114*, 7268−7316.
(7) Pophale, R.; Cheeseman, P. A.; Deem, M. W. *Phys. Chem. Chem. Phys.* **2011**, *13*, 12407−12412.
(8) Foster, M. D.; Delgado Friedrichs, O.; Bell, R. G.; Almeida Paz, F. A.; Klinowski, J. *J. Am. Chem. Soc.* **2004**, *126*, 9769−9775.
(9) Dědeček, J.; Sobalík, Z.; Wichterlová, B. *Catal. Rev.: Sci. Eng.* **2012**, *54*, 135−223.
(10) Ogura, M.; Itabashi, K.; Dedecek, J.; Onkawa, T.; Shimada, Y.; Kawakami, K.; Onodera, K.; Nakamura, S.; Okubo, T. *J. Catal.* **2014**, *315*, 1−5.
(11) Zhang, L.; Chen, K.; Chen, B.; White, J. L.; Resasco, D. E. *J. Am. Chem. Soc.* **2015**, *137*, 11810−11819.
(12) Gardner, D. W.; Huo, J.; Hoff, T. C.; Johnson, R. L.; Shanks, B. H.; Tessonnier, J.-P. *ACS Catal.* **2015**, *5*, 4418−4422.
(13) Bhan, A.; Iglesia, E. *Acc. Chem. Res.* **2008**, *41*, 559−567.
(14) Gounder, R.; Iglesia, E. *J. Am. Chem. Soc.* **2009**, *131*, 1958−1971.
(15) Román-Leshkov, Y.; Moliner, M.; Davis, M. E. *J. Phys. Chem. C* **2011**, *115*, 1096−1102.
(16) Yoshioka, M.; Yokoi, T.; Tatsumi, T. *ACS Catal.* **2015**, *5*, 4268−4275.
(17) Sklenak, S.; Dědeček, J.; Li, C.; Wichterlová, B.; Gábová, V.; Sierka, M.; Sauer, J. *Angew. Chem., Int. Ed.* **2007**, *46*, 7286−7289.
(18) Vjunov, A.; Fulton, J. L.; Huthwelker, T.; Pin, S.; Mei, D.; Schenter, G. K.; Govind, N.; Camaioni, D. M.; Hu, J. Z.; Lercher, J. A. *J. Am. Chem. Soc.* **2014**, *136*, 8296−8306.
(19) Brus, J.; Kobera, L.; Schoefberger, W.; Urbanová, M.; Klein, P.; Sazama, P.; Tabor, E.; Sklenak, S.; Fishchuk, A. V.; Dědeček, J. *Angew. Chem., Int. Ed.* **2015**, *54*, 541−545.

DOI: 10.1021/jacs.6b01341
J. Am. Chem. Soc. 2016, 138, 6184−6193

(20) Navrotsky, A.; Trofymluk, O.; Levchenko, A. A. *Chem. Rev.* **2009**, *109*, 3885−3902.
(21) Navrotsky, A. *Proc. Natl. Acad. Sci. U. S. A.* **2004**, *101*, 12096−12101.
(22) Navrotsky, A.; Tain, Z.-R. *Chem. - Eur. J.* **2001**, *7*, 769−774.
(23) Kamakoti, P.; Barckholtz, T. A. *J. Phys. Chem. C* **2007**, *111*, 3575−3583.
(24) Odoh, S. O.; Deem, M. W.; Gagliardi, L. *J. Phys. Chem. C* **2014**, *118*, 26939−26946.
(25) Montejo-Valencia, B. D.; Curet-Arana, M. C. *J. Phys. Chem. C* **2015**, *119*, 4148−4157.
(26) Zwijnenburg, M. A.; Bromley, S. T. *Phys. Chem. Chem. Phys.* **2010**, *12*, 14579−14584.
(27) Catlow, R.; Bell, R.; Cora, F.; French, S. A.; Slater, B.; Sokol, A. *Annu. Rep. Prog. Chem., Sect. A: Inorg. Chem.* **2005**, *101*, 513−547.
(28) Sanders, M. J.; Leslie, M.; Catlow, C. R. A. *J. Chem. Soc., Chem. Commun.* **1984**, 1271−1273.
(29) Schröder, K.-P.; Sauer, J.; Leslie, M.; Catlow, C. R. A.; Thomas, J. M. *Chem. Phys. Lett.* **1992**, *188*, 320−325.
(30) Bushuev, Y. G.; Sastre, G. *J. Phys. Chem. C* **2010**, *114*, 19157−19168.
(31) Li, Y.; Yu, J.; Xu, R. *Angew. Chem., Int. Ed.* **2013**, *52*, 1673−1677.
(32) Nine new noninterrupted frameworks approved by IZA after we started our computations, that is, IFW, IFY, IRN, POS, UOV, CSV, PSI, JNT, and MWF, were not included here.
(33) Gale, J. D. *J. Chem. Soc., Faraday Trans.* **1997**, *93*, 629−637.
(34) Löwenstein, W. *Am. Mineral.* **1954**, *39*, 92−96.
(35) Matsumoto, M.; Nishimura, T. *ACM Trans. Model. Comput. Simul.* **1998**, *8*, 3−30.
(36) Corma, A.; Davis, M. E. *ChemPhysChem* **2004**, *5*, 304−313.
(37) Wragg, D. S.; Morris, R. E.; Burton, A. W. *Chem. Mater.* **2008**, *20*, 1561−1570.
(38) Akporiaye, D. E.; Price, G. D. *Zeolites* **1989**, *9*, 321−328.
(39) Ghorbanpour, A.; Rimer, J. D.; Grabow, L. C. *Catal. Commun.* **2014**, *52*, 98−102.
(40) Barrer, R. M.; White, E. A. D. *J. Chem. Soc.* **1951**, 1267−1278.
(41) Zones, S. I.; Van Nordstrand, R. A. *Zeolites* **1988**, *8*, 166−174.
(42) Robson, H. *Verified Syntheses of Zeolitic Materials*, 2nd ed.; Elsevier: Amsterdam, 2001.
(43) Dent, L. S.; Smith, J. V. *Nature* **1958**, *181*, 1794−1796.
(44) Natural Zeolites Datasheets, http://www.iza-online.org/natural/.
(45) Bibby, D. M.; Dale, M. P. *Nature* **1985**, *317*, 157−158.
(46) Moteki, T.; Chaikittisilp, W.; Shimojima, A.; Okubo, T. *J. Am. Chem. Soc.* **2008**, *130*, 15780−15781.
(47) Breck, D. W. U.S. Patent 3,130,007, April 21, 1964.
(48) Iwama, M.; Suzuki, Y.; Plévert, J.; Itabashi, K.; Ogura, M.; Okubo, T. *Cryst. Growth Des.* **2010**, *10*, 3471−3479.
(49) Conato, M. T.; Oleksiak, M. D.; McGrail, B. P.; Motkuri, R. K.; Rimer, J. D. *Chem. Commun.* **2015**, *51*, 269−272.
(50) Gramlich, V.; Meier, W. M. *Z. Kristallogr. - Cryst. Mater.* **1971**, *133*, 134−149.
(51) Joshi, P. N.; Kotasthane, A. N.; Shiralkar, V. P. *Zeolites* **1990**, *10*, 598−602.
(52) Li, X.; Deem, M. W. *J. Phys. Chem. C* **2014**, *118*, 15835−15839.
(53) Newsam, J. M.; Treacy, M. M. J.; Koetsier, W. T.; De Gruyter, C. B. *Proc. R. Soc. London, Ser. A* **1988**, *420*, 375−405.
(54) Kokotailo, G. T.; Lawton, S. L.; Olson, D. H.; Meier, W. M. *Nature* **1978**, *272*, 437−438.
(55) Kamimura, Y.; Chaikittisilp, W.; Itabashi, K.; Shimojima, A.; Okubo, T. *Chem. - Asian J.* **2010**, *5*, 2182−2191.
(56) Boggs, R. C.; Howard, D. G.; Smith, J. V.; Klein, G. L. *Am. Mineral.* **1993**, *78*, 822−826.
(57) Argauer, R. J.; Landolt, G. R. U.S. Patent 3,702,886, November 14, 1972.
(58) Flanigen, E. M.; Bennett, J. M.; Grose, R. W.; Cohen, J. P.; Patton, R. L.; Kirchner, R. M.; Smith, J. V. *Nature* **1978**, *271*, 512−516.
(59) Itabashi, K.; Kamimura, Y.; Iyoki, K.; Shimojima, A.; Okubo, T. *J. Am. Chem. Soc.* **2012**, *134*, 11542−11549.
(60) Lobo, R. F.; Tsapatsis, M.; Freyhardt, C. C.; Chan, I.; Chen, C.-Y.; Zones, S. I.; Davis, M. E. *J. Am. Chem. Soc.* **1997**, *119*, 3732−3744.
(61) Plévert, J.; Kubota, Y.; Honda, T.; Okubo, T.; Sugi, Y. *Chem. Commun.* **2000**, 2363−2364.
(62) Arika, J.; Miyazaki, H.; Igawa, K.; Itabashi, K. U.S. Patent 4,650,654, March 17, 1987.
(63) Hacarlioglu, P.; Lee, D.; Gibbs, G. V.; Oyama, S. T. *J. Membr. Sci.* **2008**, *313*, 277−283.
(64) Navrotsky, A.; Geisinger, K. L.; McMillan, P.; Gibbs, G. V. *Phys. Chem. Miner.* **1985**, *11*, 284−298.
(65) O'Keeffe, M.; Hyde, B. G. *Crystal Structures I: Patterns and Symmetry*; Mineralogical Society of America: Washington, DC, 1996.
(66) Nicholas, J. B.; Winans, R. E.; Harrison, R. J.; Iton, L. E.; Curtiss, L. A.; Hopfinger, A. J. *J. Phys. Chem.* **1992**, *96*, 10247−10257.
(67) Sartbaeva, A.; Wells, S. A.; Treacy, M. M. J.; Thorpe, M. F. *Nat. Mater.* **2006**, *5*, 962−965.
(68) Dedecek, J.; Balgová, V.; Pashkova, V.; Klein, P.; Wichterlová, B. *Chem. Mater.* **2012**, *24*, 3231−3239.
(69) Yokoi, T.; Mochizuki, H.; Namba, S.; Kondo, J. N.; Tatsumi, T. *J. Phys. Chem. C* **2015**, *119*, 15303−15315.
(70) Sazama, P.; Tabor, E.; Klein, P.; Wichterlova, B.; Sklenak, S.; Mokrzycki, L.; Pashkkova, V.; Ogura, M.; Dedecek, J. *J. Catal.* **2016**, *333*, 102−114.
(71) Chen, J.; Liang, T.; Li, J.; Wang, S.; Qin, Z.; Wang, P.; Huang, L.; Fan, W.; Wang, J. *ACS Catal.* **2016**, *6*, 2299−2313.
(72) Rajan, K. *Informatics for Materials Science and Engineering: Data-driven Discovery for Accelerated Experimentation and Application*; Butterworth-Heinemann: Oxford, 2013.

DOI: 10.1021/jacs.6b01341
J. Am. Chem. Soc. 2016, 138, 6184−6193